Journal of The Electrochemical Society, **158** (12) H1293-H1296 (2011)
0013-4651/2011/158(12)/H1293/4/$28.00 © The Electrochemical Society

Hybrid Photovoltaic Device Based on Nanoporous GaAs by Using Ag Metal-Assisted Nanoscale Lithography

Cheng-Chiang Chen and Lung-Chien Chen[*,z]

Department of Electro-Optical Engineering, National Taipei University of Technology, Taipei 106, Taiwan

This study presents a hybrid photovoltaic (PV) solar cell consisting of zinc phthalocyanine (ZnPc) on nanoporous gallium arsenide (GaAs) substrates (NPGSs). NPGSs with a low reflectivity are prepared by metal-assisted nanoscale lithography. Au nanoparticles (GNPs) are introduced into the nanoporous structure in organic/inorganic hybrid solar cells to enhance the perfonance of photovoltaic devices. The optimal measured parameters of the PV cell with the ITO/ZnPc + I_2 + PMMA (ZIP)/GNPs/NPGS/In structure are J_{sc}, V_{oc}, fill factor (FF), and power convert efficiency (PCE), which have values of 2.48 mA/cm^2, 0.55 V, 0.197, and 2.69%, respectively, under irradiation by a 100 W xenon lamp.
 [DOI: 10.1149/2.087112jes]

Manuscript submitted July 6, 2011; revised manuscript received August 30, 2011. Published November 14, 2011.

Organic/inorganic hybrid-structured solar cells are promising for application in PV system owing to their low temperature and easy fabrication.[1–9] In organic materials, zinc phthalocyanine (ZnPc) has been extensively studied as organic materials for device applications, including gas sensors, solar cells, and electroluminescence devices, owing to its easy synthesization, non-toxicity to the surrounding, strong absorption in the visible portion of the solar spectrum, and electroluminescence properties.[10–15] Therefore, in this study, a p-n junction solar cell with n-type NPGS is constructed using ZnPc as a p-type absorption layer.

Light trapping is an effective means of increasing the efficiency of solar cells. Therefore, low antireflection is essential for manufacturing highly efficient solar cells. Despite the availability of silicon-based solar cells with a porous antireflective layer,[16,17] organic/inorganic hybrid solar cells based on GaAs substrate with a light trapping layer have not been studied. A previous study described the characteristic photoluminescence of GaAs porous structures that are: produced by polarization of the substrate in HCl solution.[18] Nanostructured GaAs hole arrays were also fabricated by either anodization in NH_4OH solution or use of a focused ion beam.[19,20] On the other hand, another study suggested Ag-metal-assisted chemical etching on p-Si to produce solar cells that are more efficient than those constructed from conventional alkaline-treated Si wafers.[21] Therefore, this study demonstrated the feasibility of conducting metal-assisted chemical etching of GaAs substrate by using HF + H_2O_2 + $AgNO_3$ solution, as well as its effectiveness. The optical properties of nanoporous GaAs substrates (NPGSs) prepared by metal-assisted nanoscale lithography are also investigated, as well as the characteristics of the solar cells with NPGS/ZnPc + I_2 + PMMA (ZIP) hybrid structure.

Experimental

Single crystalline (100) n-type GaAs substrates with a resistivity of 10 Ω-cm were used in this work. In the metallization step, Ag nanoparticles were deposited on GaAs substrates by immersion in 1.11 M HF and 4.7×10^{-2} M $AgNO_3$ metallization aqueous solution to form a nanoscale mask. Following electroless metallization, the substrates were etched in aqueous solutions containing HF, H_2O_2, and deionized (DI) water at volume ratios of 8:7:5 for various etching times to form an NPGS. The Au nanoparticles (GNPs) with sizes of approximately 20 nm were formed on the GaAs substrate with a nanoporous structure by an immersion method at 120°C. According to previous studies, GNPs facilitate the generation of charge carriers and increase the photocurrent.[22–24] As for the organic materials, ZnPc were dissolved in a tetrahydrofuran solution (50 mL), in which ZnPc (0.5 g), poly (methyl methacrylate) (PMMA) (0.2 g), and I_2 (0.2 g) were mixed with a magnetic stirrer at room temperature, and were deposited on the front side of the GaAs substrate by spin coating to form an ZnPc + I_2 + PMMA (ZIP) film with a thickness of around 200 nm. Figure 1 shows the schematic cross section of the complete hybrid solar cell structure. The resulting morphologies were evaluated by field emission scanning electron microscopy (FESEM). The integrated total reflectance was measured at a nearly 0° and 45° incident angle using an optical spectrometer (Hitachi U-4100). Additionally, the current density–voltage (J-V) characteristics were determined using a Keithley 2420 programmable source meter under irradiation by a 100 W xenon lamp. Finally, the irradiation power density on the surface of the sample was calibrated as 100 W/m^2.

Results and Discussion

Figure 2 shows the FESEM morphological images of the GaAs substrate with various etching times. Remaining Ag nanoparticles were observed, as shown in Fig. 2a, The Ag nanoparticles remaining on the surface of the GaAs substrate is from the dissolved $AgNO_3$. Following metallization, when an Ag-loaded GaAs substrate is immersed in an aqueous solution of HF and H_2O_2, gas evolving is observed together with time-evolution interferential colors at the beginning of the treatment. The first stages of the etching are investigated by using FESEM.

In less than 10 min, the Ag nanoparticles sink into the GaAs substrate; in addition, pore openings with a diameter similar to that of the nanoparticles are observed, as shown in Fig. 2a. The pore density is identical to the nanoparticle density. For an etching time exceeding 15 min, the pore openings are larger and less clearly defined, indicating a progressive dissolution of the GaAs walls at the surface, as shown in Fig. 2b. The color changes are most likely owing to the formation of a porous GaAs layer with a lower refractive index than that of GaAs bulk.[25,26] According to Fig. 2c, metal-assisted chemical etching results in a regular array of inverted pyramidal pits with facets at 38° to the horizontal plane owing to the anisotropic etching properties of GaAs in aqueous solution of HF-H_2O_2. Notably, {111} facets develop, as the {111} planes are etched more slowly than other crystalline planes.

Figure 3 plots the reflectivity of samples with various etching times, while Figs. 3a and 3b show the reflectivity spectra measured at nearly 0° and 45° incident angles, respectively. According to Fig. 3a, the reflection spectrum of GaAs substrate with etching for 5 min is ∼ 35% in the range of 500 ∼ 600 nm, which is the strongest flux of solar irradiation. The reflectivities are around 10% after etching for 10 and more than 10 min. According to Fig. 3b, the reflection spectrum of GaAs substrate with etching for 5 min is ∼ 30% in the range of 500 ∼ 600 nm. The reflectivities decrease to around 10–20% after etching for 10 to 20 min.

The polished GaAs wafer is also evaluated for comparison with the samples in this work. Reflectivity of the substrate without etching, i.e. a polished surface, is high, and it decreases with an increasing etching time. The value of the integrated total reflectance from the NPGS

* Electrochemical Society Active Member.
z E-mail: oceam@ntut.edu.tw

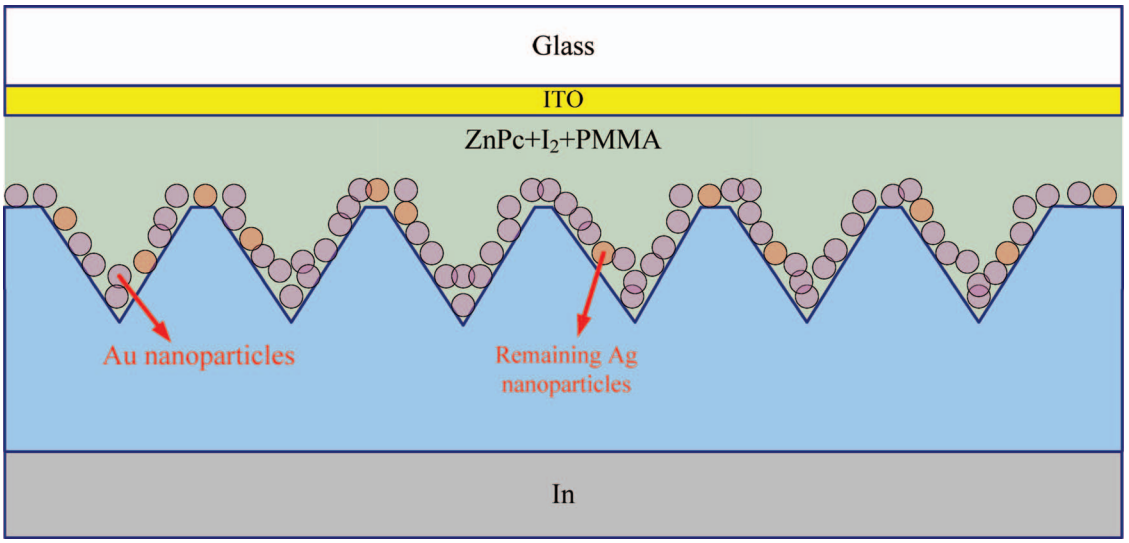

Figure 1. Schematic cross section of the complete hybrid solar cell structure.

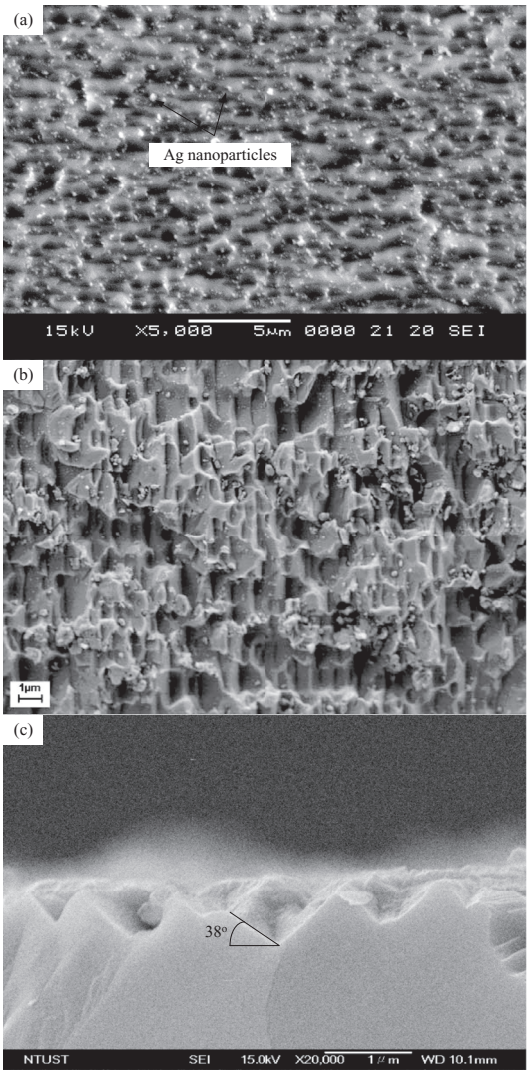

Figure 2. FESEM plan view images of a Ag loaded the porous GaAs layer produced by HF–H_2O_2 etching (8:7:5) after (a) 5 min and (b) 15 min. (c) FESEM cross section image of Fig. 2b.

formed when using HF/H_2O_2/$AgNO_3$ solution etching for 20 min is lower than around 10% over all visible wavelengths. The reflectivity changes are most likely owing to the formation of a nanoporous GaAs layer with a lower refractive index than that of GaAs bulk.[25,26]

Figure 4 shows the representation of the optical absorption measurements for ZnPc films with different dopants. Previous works have attempted to improve the optical absorbance and carrier mobility of ZnPc films by using a polymeric matrix such as PMMA.[27,28] The low absorption may be attributed mainly to its low solubility in solvents, resulting in molecular aggregation both in a solution and in the solid state causing a drastic decay of optical properties. The ZnPc + I_2 + PMMA (ZIP) films yield a higher absorption than that of ZnPc + PMMA films. The ZIP film displays the highest absorbance at wavelengths of 400 and 680 nm owing to the I_2. I_2-doped ZnPc having a better conductivity and mobility than those of undoped ZnPc.[28]

Figure 5 plots the J-V characteristics of the photovoltaic organic/inorganic hybrid-structured solar cells on the NPGS structure by the solution etching for various time intervals. The cell has an active area of 0.1 × 0.2 cm^2. Table I lists the characteristic parameters of these devices. The measured short-circuit current density (J_{sc}), open-circuit voltage (V_{oc}), fill factor (FF), and power convert efficiency (η) of the ITO/ZIP/NPGS/In organic/inorganic hybrid-structured solar cells are 2.24 mA/cm^2, 0.54 V, 0.177, and 2.14%, respectively, under irradiation by a 100 W xenon lamp. The J_{sc} of the NPGS increases for the following two reasons: (i) The NPGS with a larger effective surface area than that of GaAs substrate provides fast and direct pathways to increase the collection and transport of charge carriers. (ii) J_{sc} can be expressed as[29]

$$J_{sc} = q \int_{\lambda_2}^{\lambda_1} F(\lambda)\,[1 - R(\lambda)]\,Q_i(\lambda)d\lambda \qquad [1]$$

Table I. Parameters of organic/inorganic hybrid-structured solar cells with etching for various time intervals.

Sample	Deposition Time/Etching Time (min)	Jsc (mA/cm^2)	Voc (V)	F.F.	η (%)
EG00	0/0	0.817	0.54	0.206	0.912
EG55	5/5	0.995	0.54	0.26	1.38
EG510	5/10	1.52	0.56	0.199	1.7
EG515	5/15	1.65	0.56	0.205	1.9
EG520	5/20	2.24	0.54	0.177	2.14

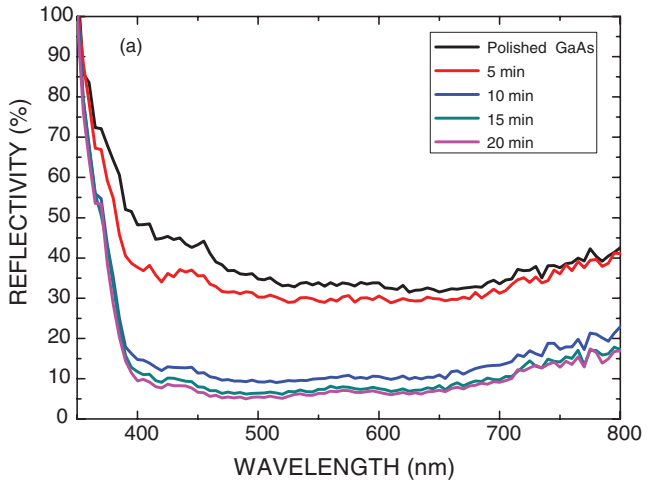

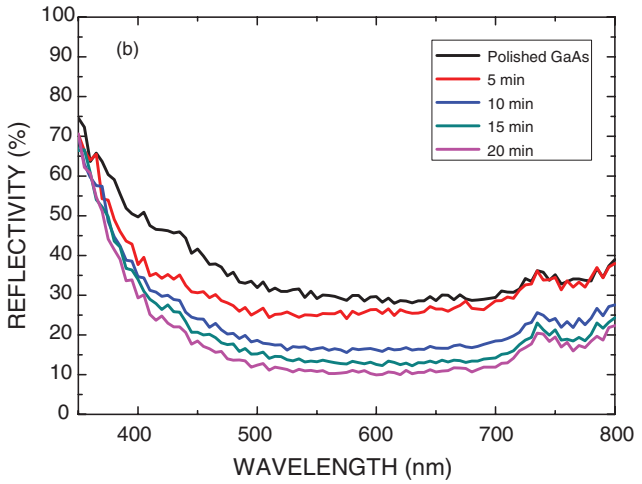

Figure 3. Reflectivity of samples with various etching times (a) nearly 0° specular reflection and (b) 45° specular reflection

where q is the electronic charge; λ_1 and λ_2 are the wavelength limits (350–1100) nm; F(λ) is the photon flux of the solar spectrum; and Q(λ) is the internal quantum efficiency. Surface of the NPGS has a lower refractive index than that of GaAs substrate.[25,26] Thus, NPGS also causes light trapping and increases short-circuit current density.

Figure 6 plots the J-V characteristics of photovoltaic organic/inorganic hybrid-structured solar cells on the NPGS structure with GNPs by performing solution etching for 20 min. The cell has an active area of 0.1 × 0.2 cm^2. Table II lists the characteristic parameters of these devices with and without GNPs introduced. The measured short-circuit current density (J_{sc}), open-circuit voltage (V_{oc}), fill factor (FF), and power convert efficiency (η) of the ITO/ZIP/GNPs/NPGS/In organic/inorganic hybrid-structured solar cells are 2.48 mA/cm^2, 0.55 V, 0.197, and 2.69%, respectively, under irradiation by a 100 W xenon lamp. GNPs and the remaining Ag nanoparticles facilitates the generation of charge carriers and increases both the photocurrent and the power conversion efficiency owing to the electron quick shuttling effect.[22–24]

Table II. Parameters of organic/inorganic hybrid-structured solar cells with and without GNPs.

Dope GNP	Jsc (mA/cm^2)	Voc (V)	F.F.	η (%)
ZIPT-EG520 GaAs	2.24	0.54	0.177	2.14
ZIPT-GNP-EG520 GaAs	2.48	0.55	0.197	2.69

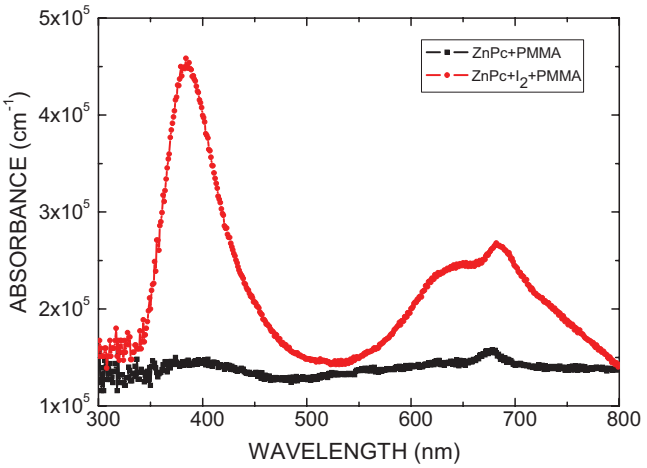

Figure 4. Absorbance spectra of ZnPc films with various dopants.

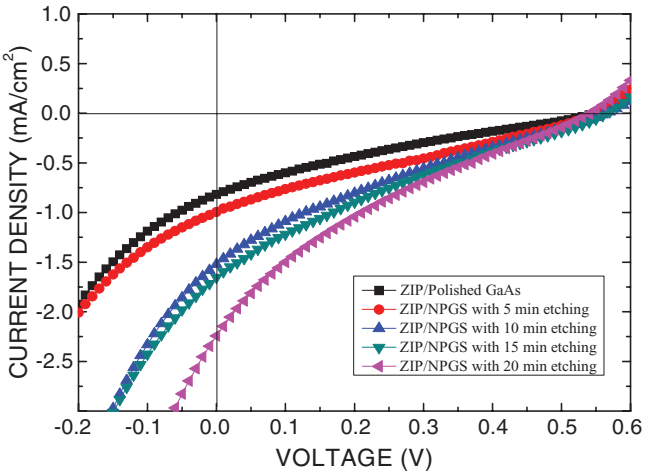

Figure 5. J-V characteristics of the organic/inorganic hybrid-structured solar cells on the NPGS structure by the solution etching for various time intervals.

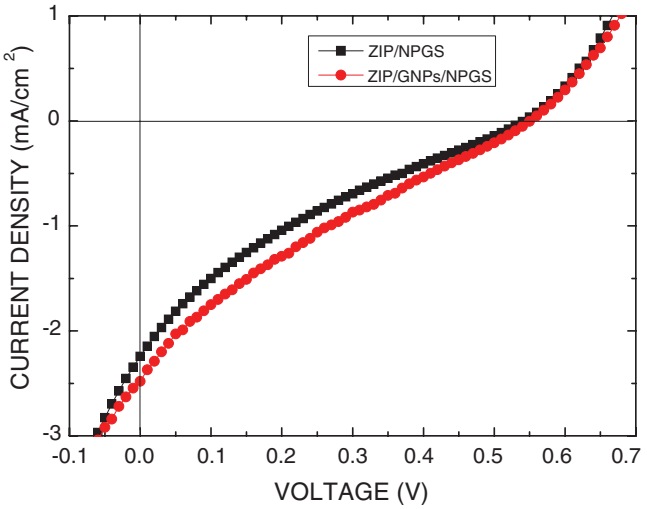

Figure 6. J-V characteristics of the organic/inorganic hybrid-structured solar cells with different structures under illumination.

Conclusions

This study investigated the feasibility of preparing an NPGS based on metal-assisted nanoscale lithography. Organic/inorganic hybrid solar cells with GNPs, and ZIP on NPGS structure were also studied. The measured parameters of the solar cell with the ITO/ZIP/GNPs/NPGS/In structure were J_{sc}, V_{oc}, FF, and power convert efficiency, which had values of 2.48 mA/cm^2, 0.55 V, 0.197, and 2.69%, respectively. Experimental results indicate that GNPs and Ag nanoparticles facilitate the generation of charge carriers and increase both the photocurrent and the power conversion efficiency owing to the electron quick shuttling effect. However, the cells have poor power conversion efficiency and a low fill factor may be attributed to the leakage of photo-generated carrier. Another factor is probably a high resistance from oxide on the surface of NPGS due to chemical etching.

Acknowledgment

Financial support of this work was provided by the National Science Council of the Republic of China under Contract No. NSC 99-2221-E-027-061

References

1. F. C. Krebs, *Sol. Energy Mater. Sol. Cells*, **93**, 394 (2009).
2. F. C. Krebs, M. Jørgensen, K. Norrman, O. Hagemann, J. Alstrup, T. D. Nielsen, J. Fyenbo, K. Larsen, and J. Kristensen, *Sol. Energy Mater. Sol. Cells*, **93**, 422 (2009).
3. F. C. Krebs, S. A. Gevorgyan, and J. Alstrup, *J. Mater. Chem.*, **19**, 5442 (2009).
4. F. C. Krebs, *Sol. Energy Mater. Sol. Cells*, **93**, 465 (2009).
5. F. C. Krebs, *Sol. Energy Mater. Sol. Cells*, **93**, 1636 (2009).
6. F. C. Krebs, *Org. Electron.*, **10**, 761 (2009).
7. C. N. Hoth, S. A. Choulis, P. Schilinsky, and C. J. Brabec, *Adv. Mater.*, **19**, 3973 (2007).
8. T. Aernouts, T. Aleksandrov, C. Girotto, J. Genoe, and J. Poortmans, *Appl. Phys. Lett.*, **92**, 033306 (2008).
9. M. D. McGehee, *MRS Bull.*, **34**, 95 (2009).
10. C. C. Leznoff and A. B. P. Lever, *Phthalocyanine-Properties and Applications*, Vol. 3, VCH, New York, (1993).
11. G. Winter, H. Heckmann, P. Haisch, W. Eberhard, and M. Hanack, *J. Am. Chem. Soc.*, **120**, 11663 (1998).
12. Z. L. Yang, H. Z. Chen, L. Cao, H. Y. Li, and M. Wang, *Mater. Sci. Eng.*, **B 106**, 73 (2004).
13. S. Y. Al-Raqa, A. S. Solieman, A. A. Joraid, S. N. Alamri, Z. Moussa, and A. Aljuhani, *Polyhedron*, **27**, 1256 (2008).
14. R. Sathyamoorthy, S. Senthilarasu, S. Lalitha, A. Subbarayan, K. Natarajan, and X. Mathew, *Sol. Eng. Mat. Sol. Cells*, **82**, 169 (2004).
15. L. C. Chen, C. C. Wang, and C. B. Cheng, *Thin Solid Films*, **517**, 1790 (2009).
16. J. Kim, *J. Korean Phys. Soc.*, **50**, 1168 (2007).
17. L. Schirone, G. Sotgiu, and F. P. Califano, *Thin Solid Films*, **297**, 296 (1997).
18. P. Schmuki, D. J. Lockwood, H. J. Labbé, and J. W. Fraser, *Appl. Phys. Lett.*, **69**, 1620 (1996).
19. Y. Morishita, J. Sunagawa, Y. Yumoto, and S. Kawai, *J. Cryst. Growth*, **227–228**, 1049 (2001).
20. Y. Morishita, M. Ishiguro, S. Miura, and Y. Enmei, *J. Cryst. Growth*, **237–239**, 1291 (2002).
21. K. Tsujino, M. Matsumura, and Y. Nishimoto, *Sol. Energy Mater. Sol. Cells*, **90**, 100 (2006).
22. S. W. Tong and C. F. Zhang, *Chem. Phys. Lett.*, **453**, 73 (2007).
23. C. Hagglund, M. Zäch and B. Kasemo, *Appl. Phys. Lett.*, **92**, 013113 (2008).
24. S. Barazzouk and S. Hotchandani, *J. Appl. Phys.*, **96**, 7744 (2004).
25. L. Yang, J. Motohisa, T. Fukui, L. X. Jia, L. Zhang, M. M. Geng, P. Chen, and Y. L. Liu, *Optics Express*, **17**, 9337 (2009).
26. S. R. Kisting, P. W. Bohn, E. Andideh, I. Adesida, B. T. Cunningham, and T. D. Harris, *Appl. Phys. Lett.*, **57**, 1328 (1990).
27. R. Ostuni, M. C. Larciprete, G. Leashu, A. Belardini, C. Sibilia, and M. Bertolotti, *J. Appl. Phys.*, **101**, 033116 (2007).
28. L. C. Chen and C. N. Pan, *Eur. Phys. J.: Appl. Phys.*, **44**, 43 (2008).
29. M. Cid, N. Stem, C. Brunetti, A. F. Beloto, and C. A. S. Ramos, *Surf. Coat. Technol.*, **106**, 117 (1998).